NEUROSCIENCE
RESEARCH ARTICLE
A. E. Edwards et al. / Neuroscience 395 (2018) 35–48

Electroencephalographic Correlates of Continuous Postural Tasks of Increasing Difficulty

Amy E. Edwards,[†] Onur Guven,[†] Michael D. Furman, Qadeer Arshad[††] and Adolfo M. Bronstein*[††]

Neuro-otology Unit, Division of Brain Sciences, Imperial College London, Charing Cross Hospital, London, UK

Abstract—Cortical involvement in postural control is well recognized, however the role of non-visual afferents remains unclear. Parietal cortical areas are strongly implicated in vestibulo-spatial functions, but topographical localization during balance tasks remains limited. Here, we use electroencephalography (EEG) during continuous balance tasks of increasing difficulty at single electrode positions. Twenty-four healthy, right-handed individuals performed four balance tasks of increasing difficulty (bipedal and unipedal) and a seated control condition with eyes closed. Subjective ratings of task difficulty were obtained. EEG was recorded from 32 electrodes; 5 overlying sensory and motor regions of interest (ROIs) were chosen for further investigation: C3, Cz, C4, P3, P4. Spectral power and coherence during balance tasks were analyzed in theta (4–8 Hz) and alpha (8–12 Hz) bands. Alpha power reduced as task difficulty increased and this reduction correlated with subjective difficulty ratings. Alpha coherence increased with task difficulty between C3–Cz–C4 electrode pairs. Differential changes in power were observed in Cz, suggestive of a distinct role at this electrode location, which captures lower limb cortical representation. Hemispheric asymmetry was observed, as reflected by greater reductions in theta and alpha power in right-sided areas. Our results demonstrate the functional importance of bilateral central and parietal cortices in continuous balance control. The hemispheric asymmetry observed implies that the non-dominant hemisphere is involved with online monitoring of postural control. Although the posterior parietal asymmetry found may relate to vestibular, somatosensory or multisensory feedback processing, we argue that the finding relates to active balance control rather than simple sensory-intake or reflex circuit activation.

Key words: postural control, continuous balance, hemispheric asymmetry, parietal cortex, EEG, coherence.

INTRODUCTION

Postural control requires the integration of visual, vestibular and proprioceptive sensory cues (Maurer et al., 2000) and was historically understood to involve only subcortical, spinal and cerebellar structures (Magnus, 1926; Keck et al., 1998). While cortical involvement in postural control is now unequivocally accepted, based partly on electroencephalography (EEG) data, (Ouchi et al., 1999; Jacobs and Horak, 2007; Mihara et al., 2008; Slobounov et al., 2008; Slobounov et al., 2009; Bolton et al., 2012; Sipp et al., 2013; Varghese et al., 2014; Hülsdünker et al., 2015; Hülsdünker et al., 2016), its exact role remains unclear. It has been suggested that even in stable balance, cortical involvement may increase with age due to deteriorations in subcortical control loops (Baudry, 2016; Ozdemir et al., 2018).

Attempts to separate multimodal sensory contributions to balance control have been limited to the exclusion of visual input (eye closure) (Slobounov et al., 2009; Tse et al., 2013; Hülsdünker et al., 2015; Varghese et al., 2015; Ozdemir et al., 2018). Differences between somatosensory, proprioceptive and vestibular cortical contributions remain unexplored (Bolton, 2015), perhaps in part due to the complexity of deciphering vestibular and proprioceptive cortices (Brandt, 2003). Despite this difficulty, studies aiming to identify cortical areas involved with vestibular processing have repeatedly implicated parietal areas (Fasold et al., 2002; Kahane et al., 2003; Lopez et al., 2012), with recent work additionally demonstrating their functional importance in maintaining spatial orientation (Arshad et al., 2013; Arshad et al., 2014; Kaski et al., 2016). Similarly, proprioceptive cortical processing involves parietal areas and is functionally

*Corresponding author. Address: Neuro-otology Unit, Division of Brain Sciences, Imperial College London, Charing Cross Hospital, London W6 8RF, UK.
E-mail addresses: amy.edwards15@imperial.ac.uk (A. E. Edwards), o.guven11@imperial.ac.uk (O. Guven), q.arshad@imperial.ac.uk (Q. Arshad), a.bronstein@imperial.ac.uk (A. M. Bronstein).
[†] Contributed equally.
[††] Contributed equally.

Abbreviations: (f)MRI, (functional) magnetic resonance imaging; ANOVA, analysis of variance; EEG, electroencephalography/electroencephalographic; EMG, electromyography/electromyographic; FFT, Fast Fourier Transform(ation); FIR, finite impulse response; ROI(s), region(s) of interest; r_s, rho (Spearman correlation coefficient).

https://doi.org/10.1016/j.neuroscience.2018.10.040
0306-4522/

relevant for postural control (Pellijeff et al., 2006; Limanowski and Blankenburg, 2016).

Unlike functional Magnetic Resonance Imaging (fMRI), EEG can be applied during upright posture and has therefore dominated studies investigating cortical control of balance. EEG also offers high temporal resolution, meaning that most research to date has focussed on event-related changes and transient postural perturbations (Slobounov et al., 2005; Adkin et al., 2006; Slobounov et al., 2009; Tse et al., 2013; Varghese et al., 2014; Varghese et al., 2015). While the latter are useful to understand responses to transient balance disturbance, such brief changes are unlikely to be representative of mechanisms involved in maintaining continuous balance. Quite apart from any theoretical implications, understanding EEG patterns during a range of standing postures of varying difficulty will pave the way for the EEG study of clinical conditions in which patients experience sensations of dizziness or unsteadiness only when upright, but without major alterations of postural reflexes (Ahmad et al., 2015; Kim et al., 2015; Schöberl et al., 2017; Nigro et al., 2018).

Continuous balance has only recently been investigated using EEG (Hülsdünker et al., 2015; Hülsdünker et al., 2016; Ozdemir et al., 2018). Theta (4–8 Hz) power is reported to rise with increasing balance demand in parietal areas (Hülsdünker et al., 2015; Hülsdünker et al., 2016), as well as in frontal areas (Sipp et al., 2013; Slobounov et al., 2013; Varghese et al., 2014). Lower centro-parietal theta activity is found to be associated with better task performance, thus theta oscillations have been suggested to represent error detection and processing during postural maintenance (Slobounov et al., 2009; Hülsdünker et al., 2015). Reduction in lower alpha power (8–10 Hz) with greater task difficulty has also been demonstrated, suggested to reflect increased thalamo-cortical information transfer and generalized cortical activation (Hülsdünker et al., 2016). Alpha oscillations have been implicated in attentional aspects of balance control, particularly visuo-spatial attention (Ray and Cole, 1985; Rihs et al., 2007). Increases in central and centro-parietal delta (0.2–4 Hz) activity have been reported separately, however these were interpreted as related to lower limb movement planning and execution, rather than tasks involved in quiet postural maintenance (Ozdemir et al., 2018). Although increases in slow wave (delta and/or theta) activity may seem counter-intuitive, particularly taking into consideration observations made in the clinical EEG setting (Scott, 1976; Britton et al., 2016), increases in delta and theta power with task complexity have been demonstrated in multiple contexts, including visuo-motor tasks (Slobounov et al., 2000; Gomarus et al., 2006) and with increasing cognitive load (Harmony et al., 1996; Gevins and Smith, 2000).

Although spectral changes during different balance tasks have been demonstrated in various frequency bands, spatial resolution of existing studies has been limited (Hülsdünker et al., 2015; Hülsdünker et al., 2016; Ozdemir et al., 2018). Spatial resolution is a recognized issue of EEG; however, it has been further compromised in these analyses by the grouping of electrodes over both hemispheres. This was particularly the case for central and parietal areas, which are known to be important in relation to efferent (lower limb motor) and afferent (vestibular and proprioceptive) aspects of balance, respectively (Kalaska et al., 1990; Wang et al., 2006; zu Eulenburg et al., 2012; Arshad et al., 2014), particularly over the non-dominant (right) hemisphere (Dieterich et al., 2003a; Janzen et al., 2008; Pérrenou et al., 2008; Arshad et al., 2015).

The purpose of this study was to characterize changes in cortical activity associated with continuous, steady-state balance control in healthy individuals at single (rather than grouped) electrode positions. Balance task difficulty was quantified to enable correlation with spectral power. Electrodes chosen in our regions of interest (ROIs) were C3, Cz and C4, approximately overlying the medial aspects of the primary motor cortex bilaterally (lower limb areas) and P3 and P4, which may capture activity from Brodmann areas 39, 40 and 7 (involved with vestibular and proprioceptive information processing) (Homan et al., 1987; Kahane et al., 2003; Okamoto et al., 2004; Koessler et al., 2009; Trans Cranial Technologies, 2012). Eyes remained closed throughout to exclude visual input and maximize vestibular and proprioceptive afferent contribution to balance maintenance. Theta (4–8 Hz) and alpha (8–12 Hz) frequency bands were investigated as they are recognized to be involved in balance control (Pfurtscheller et al., 2000; Adkin et al., 2006; Slobounov et al., 2008; Del Percio et al., 2009; Slobounov et al., 2009; Sauseng et al., 2013; Sipp et al., 2013; Varghese et al., 2014) and are least vulnerable to signal artifact.

EXPERIMENTAL PROCEDURES

Study participants

Twenty-four, right hand and right foot dominant, healthy volunteers were recruited (age 22.7, SD 3.0 years; 13 female). Exclusion criteria were factors which could confound EEG data, including a personal or family history of seizures, unexplained loss of consciousness or falls, and conditions that could impair balance performance, including recent injury to either lower limb, known muscle or vestibulo-cerebellar disease, and alcohol consumption within 24 h. All subjects provided written informed consent prior to participation in compliance with the World Medical Association Declaration of Helsinki.

Experimental protocol

Each subject performed 4 balance tasks and a seated control condition, all with eyes closed. The difficulty of each balance task was determined by surface (floor vs. foam) and stance (bipedal vs. unipedal) in a 2×2 factorial design. During bipedal conditions (FLOOR, FOAM), subjects stood with their feet shoulder width apart and arms by their sides. During unipedal conditions (RFLOOR, RFOAM), subjects balanced on their right foot with arms outstretched and left leg

raised. A foam surface of 10-cm depth was used to disrupt the reliability of somatosensory afferent information. Subjects were asked only to touch their left foot to the ground if loss of balance was imminent, and to do so as briefly and infrequently as possible. These time epochs were noted and later eliminated from the analysis.

All conditions were preceded by practice runs, which were not recorded. This was to minimize potential confounding effects of motor learning and task familiarity. EEG was recorded for 2 min in the baseline seated condition before the 4 balance tasks, which were counterbalanced in order. Bipedal recordings were for 2 min and unipedal for 3 min, to allow for potential elimination of trace sections due to signal disruption and loss of balance, predicted to be more likely in unipedal tasks.

Task difficulty

Task difficulty was investigated using both subjective and objective measures. All participants were asked to rate difficulty in the seated and 4 balance tasks using a numerical scale between 1 and 5. Mean ratings (n = 24) determined that task difficulty increased in the following order: FLOOR-FOAM-RFLOOR-RFOAM [Table 1], which was corroborated by measurements of postural instability in two of the participating subjects, separate from EEG recording. In addition, 24 normal subjects (age 22.8, SD 3.2 years; 13 female) had postural instability measured and correlated with individual 1–5-point subjective ratings. An in-house-built force posturography plate was used to measure postural instability (sway path), as detailed elsewhere (Lekhel et al., 1997; Guerraz et al., 2001; Yarrow et al., 2001). This confirmed the order of task difficulty and demonstrated a strong positive correlation between rated difficulty and measured instability, Spearman rho (r_s) = 0.851 (p = 0.000). As such, all data relating to balance tasks will be presented in this order. For simplicity, correlations between EEG band power and task difficulty will be based on individual subjective ratings, as biomechanical descriptors of increased task difficulty require complicated measurements and are associated with increased complexity of the movement structure (Federolf et al., 2013).

Data acquisition

EEG was recorded from 32 scalp locations, according to the international 10–20 system, via electrodes mounted in a Waveguard™ cap (ANT Neuro, Enschede, The Netherlands). A 33rd electrode located 10% anterior to Fz (namely GND electrode, position AFz) was used as the common reference. Sampling rate was 2500 Hz and electrode impedances were kept below 5kOhm. All recordings were performed in a Faraday cage.

Data processing

EEG data were collected via Asa™ software (ANT Neuro). Each trace was visually examined and segments with movement or electromyographic (EMG) artifact were excluded from in-software transformation. Fast Fourier Transform (FFT) averaging was then applied in Asalab™ (ANT Neuro), and frequencies of interest (theta 4–8 Hz; alpha 8–12 Hz) were analyzed in Microsoft® Excel at 0.5-Hz bin resolution. This preliminary analysis was corroborated by independent, detailed analysis in MATLAB®, summarized in Fig. 1. After visual examination for artifact removal, the mean offset of each electrode was removed, and zero-phase low-pass filtering was applied using an anti-aliasing finite impulse response (FIR) filter. The cut-off frequency of this filter was defined at 100 Hz with a transition bandwidth of 25 Hz, a pass-band ripple of 0.01 and a stopband attenuation of 80 dB. This filter removed high-frequency content and prevented foldover when signals were down-sampled to 250 Hz. A zero-phase high-pass filter was then applied, using a FIR filter with a cut-off frequency and a transition bandwidth of 0.5 Hz, a pass-band ripple of 0.01 and a stopband attenuation of 60 dB. Stopband attenuations were selected only as high as required, to maximize computational efficiency (Widmann and Schröger, 2012; Widmann et al., 2015). Finally, a zero-phase notch filter removed powerline interference. FFT was then performed, and theta and alpha band power calculated for ROIs. The outputs of preliminary [Figs. 2 and 3] and more detailed analyses [Fig. 4] were identical. In addition to power analysis, magnitude-squared EEG coherence (MATLAB®) between each pair of the 5 electrodes in our ROIs was calculated for both frequency bands of interest (Babiloni et al., 2011).

Data normalization

EEG signal strength can differ greatly between individuals and between separate recordings in the same individual due to several factors including anatomo-physiological differences and impedance mismatch. Accordingly, signal data for each balance task recording were normalized by expressing the total power in each frequency band relative to the respective individual SITTING value in power analyses. These normalized data were displayed on head plots for topographical visual representation only [Fig. 4] and processed statistically (see below). Analogous normalization was applied to individual coherence values.

Statistical analysis

All statistical analysis was conducted in SPSS® Statistics 23 (IBM® Corp.). In cases where data did not meet normality criteria, non-parametric tests were used. Descriptive statistics were generated immediately after data normalization. These indicated large inter-individual variability, a recognized feature of EEG data. To improve the reliability by reducing data variance, our statistical package identified values beyond 3SD from the group mean as outliers, which were then excluded prior to any further analysis of separate frequency bands.

On the above basis, 4/24 subjects were excluded from power analysis of the theta band (n = 20) and 8/24 from analysis of the alpha band (n = 16), 2 of which were also

Table 1. Subjective difficulty ratings for control condition and four balance tasks. Mean and range (n = 24) of participant-rated task difficulty on an integer scale between 1 and 5

Task	SITTING	FLOOR	FOAM	RFLOOR	RFOAM
Mean (SD)	1 (0)	1.50 (0.51)	2.31 (0.55)	3.44 (0.65)	4.63 (0.49)
Minimum	1	1	2	2	4
Maximum	1	2	5	5	5

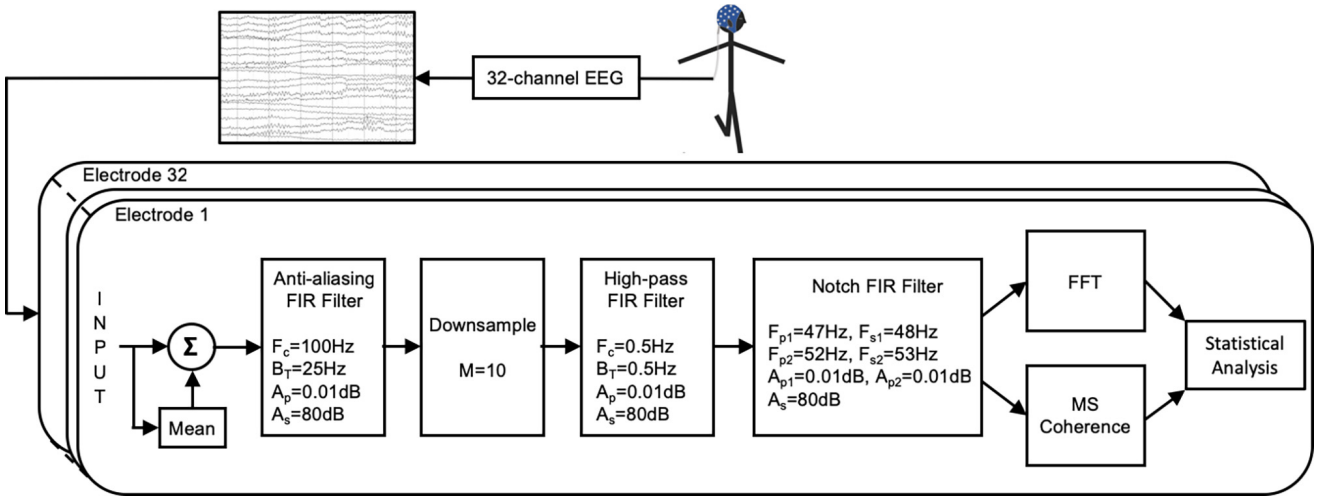

Fig. 1. Flowchart of the EEG processing steps, showing filter characteristics, down-sampling rate and transformation details. MS = magnitude-squared.

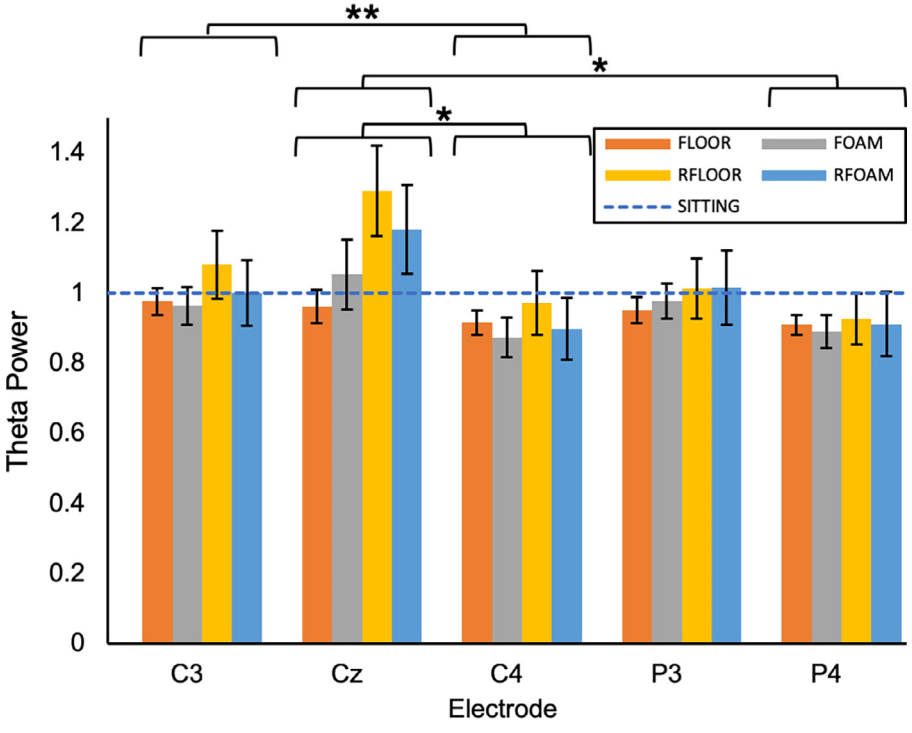

Fig. 2. Relative power in theta frequency band according to electrode and task. Each bar represents the mean relative theta power across 20 participants in a single electrode for a single condition. SITTING represented as normal line (= 1). Error bars represent standard errors of the mean (SEM). Significance levels are defined as: $p < 0.05$ (*), $p < 0.01$ (**). Post hoc analysis indicates a more prominent theta attenuation over the right hemisphere, as shown by significant asymmetries between C3–C4, Cz–C4, Cz–P4 and a similar trend for P3–P4.

among the 4/24 excluded from the separate theta band analysis. Normality was then confirmed using Shapiro-Wilk tests. A 2-way repeated measures analysis of variance (ANOVA) was performed on the normalized (relative to SITTING) power data for each frequency band using within-subject factors SITE (electrode; 5) and TASK (balance task; 4). Where the sphericity assumption was not met, Greenhouse-Geisser corrected p-values were used. Bonferroni correction was applied where multiple post-hoc comparisons were made. Pearson product-moment correlation coefficients (r) were calculated between subjective task difficulty rating and total power in each frequency band (theta and alpha) in all electrodes of interest.

A similar procedure was followed for coherence analyses in theta (n = 20) and alpha (n = 16) frequency bands. A 2-way repeated measures ANOVA was performed on absolute coherence values for each band using within-subject factors COMBINATION (3

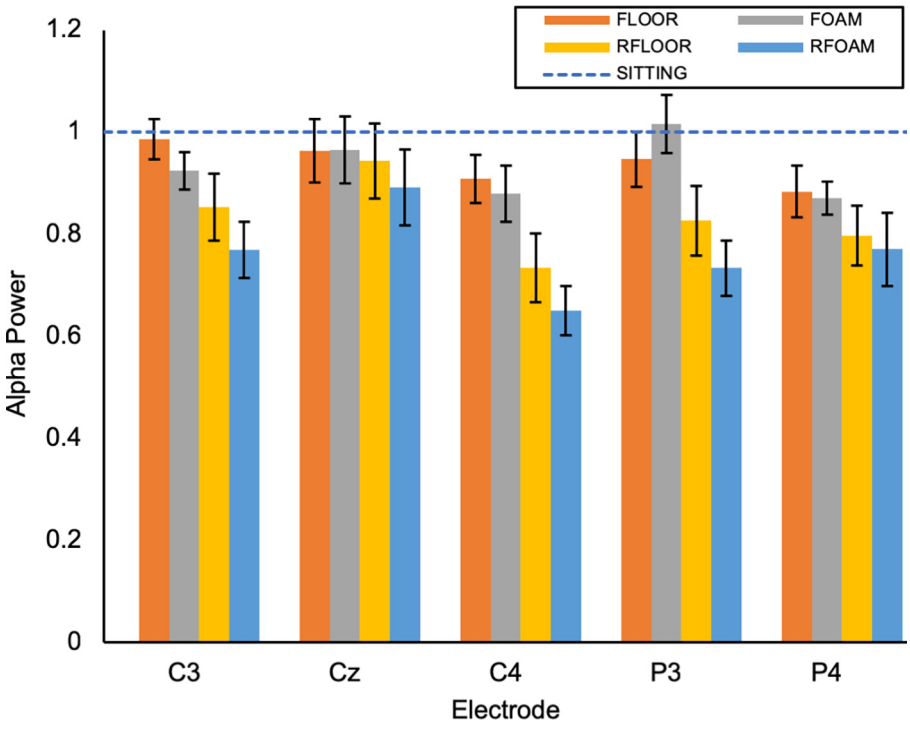

Fig. 3. Relative power in alpha frequency band according to electrode and task. Each bar represents the mean relative theta power across 16 participants in a single electrode for a single condition. SITTING represented as normal line (= 1). Note the progressive reduction in alpha power with task difficulty, from SITTING to RFOAM (ANOVA main effect of TASK: $F = 4.632$, $p = 0.025$), further explored in Fig. 6.

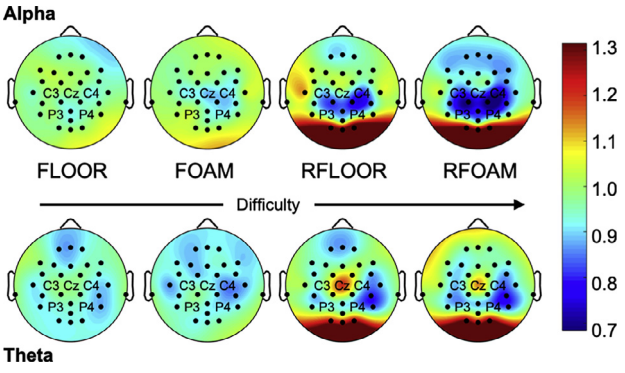

Fig. 4. Topographical maps of relative power in alpha and theta frequency bands during 4 balance tasks in 32 electrodes, top and bottom rows respectively. Each electrode is represented by a dot other than the 5 ROIs, for which labels indicate electrode position. Tasks are displayed in order of increasing difficulty from left to right, as indicated. Each head map represents mean data (alpha, $n = 16$; theta, $n = 20$) during each task. Changes in activity outside our ROIs (e.g. increase in occipital areas) have not been explored further. For illustration purposes only (i.e. not for quantitative analysis), the 32 electrode plots were subjected to Independent Component Analysis to remove frontal eye movement artifact (EEGLAB 14.1).

electrode pairing groups: central-central, central-parietal and parietal-parietal) and TASK (balance task including SITTING; 5). Where correlation between subjective task difficulty rating and coherence was investigated, coherence data were first normalized to respective SITTING values before Spearman rank-order correlation coefficients (r_s) were calculated.

RESULTS

Theta power

Fig. 2 shows the mean ($n = 20$) change in normalized power in the theta frequency band in each electrode of interest, according to balance task. There was a significant ANOVA main effect of electrode on theta power ($p = 0.003$). Post hoc analysis revealed significant differences between 3 electrode pairs: C3–C4 ($p = 0.008$), Cz–C4 ($p = 0.019$), Cz–P4 ($p = 0.043$), each representing a degree of hemispheric asymmetry, with a trend toward greater reduction in the theta frequency band in right versus left central and parietal areas. This is illustrated topographically in Fig. 4. Fig. 4 also shows a relative increase in theta power in electrode Cz during the more challenging tasks (FOAM, RFLOOR, RFOAM), greatest in RFLOOR. As this finding was topographically isolated, raw traces were visually re-examined for participants demonstrating greatest theta power increase between seated and unipedal (RFLOOR) conditions to ensure that the change was not artifactual. Examples for one individual are illustrated in Fig. 5. Cz theta increase seen in Fig. 2 could have reflected a general activity enhancement across multiple midline electrodes (Hülsdünker et al., 2015), however as shown in Fig. 4, theta power increases during the more demanding tasks fairly selectively in the central electrode Cz.

Figs. 2 and 4 suggest a slight reduction in theta power during the postural tasks in C3, C4, P3 and P4, however there was no main effect of balance task on theta power, and no correlation between subjective task difficulty and theta band power in any electrode.

Alpha power

Fig. 3 shows the mean ($n = 16$) change in normalized power in the alpha frequency band in each electrode of interest, according to balance task. There were significant ANOVA main effects of electrode ($p = 0.019$) and balance task ($p = 0.025$) on alpha power. There is a general trend toward reduction in alpha power in all 5 electrodes of interest with increasing task difficulty [Figs. 3 and 4]. In agreement, significant negative correlations were found between subjective difficulty ratings and alpha power in electrodes C3 ($r = -0.317$; $p = 0.011$), C4 ($r = -0.345$; $p = 0.005$), P3 ($r = -0.279$, $p = 0.025$) and P4 ($r = -0.249$, $p = 0.049$) [Fig. 6]. These correlations demonstrate

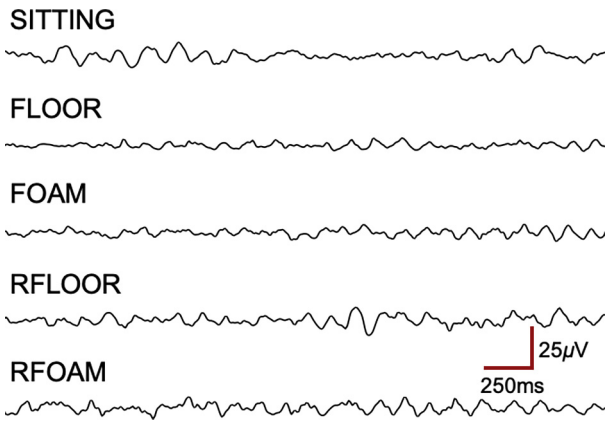

Fig. 5. Examples of raw traces from electrode Cz. Raw trace sections taken from one participant at Cz during the control condition and 4 balance tasks. There is no evidence of low-frequency artifact.

reductions in alpha power with increasing task difficulty in central and parietal regions bilaterally, albeit seen to a greater extent in right versus left cortical areas [Fig. 4].

In order to corroborate whether the posturally induced alpha reduction was localized to our ROIs, we examined surrounding electrodes. We found that the mean alpha power change in our ROIs (5 electrodes combined) was −9.00% upon balancing (4 normalized tasks combined) with respect to the seated control condition. In contrast, the electrodes surrounding our ROIs (O1, O2, Oz and POz) showed a mean change in alpha power of +5.82% and, importantly, there was no consistent modulation with balance task difficulty (mean change across electrodes and postural conditions).

In keeping with Hülsdünker et al. (2016), we observed an increase in alpha peak frequency during all postural tasks from the seated control (median SITTING alpha frequency 9.6 Hz). Median alpha peak frequency increased consistently across all five ROIs (median 2.2%, range 0.1–4.8%). As this finding is consistent with the literature it will not be discussed further.

Coherence analysis

Coherence between electrode pairs within our ROIs was measured for theta and alpha bands. Statistical analysis in the alpha band revealed a significant ANOVA main effect of electrode group ($p = 0.000$) and significant interaction between electrode group and task ($p = 0.007$), but no corresponding findings were present in the theta band. Visual inspection of the coherence values [Appendix A; Tables A.1-4] indicated that the only consistent finding was a tendency for coherence to increase with balance task difficulty between central electrode pairs in the alpha band [Fig. 7]; in agreement, significant positive correlations were found in all central pairs: C3-Cz $r_s = 0.250$ ($p = 0.025$), C3-C4 $r_s = 0.290$ ($p = 0.009$), Cz-C4 $r_s = 0.239$ ($p = 0.033$).

DISCUSSION

In this study, we used EEG to examine changes in cortical activity associated with continuous balance at single electrode positions, and correlated EEG power with subjective measures of balance difficulty. We observed a significant reduction in alpha power as balance task becomes increasingly difficult. Theta activity increased in Cz during the postural tasks. It is unlikely that our main findings (i.e. reduced power) are attributable to EMG or movement artifact, which would be expected to increase with task difficulty. Additionally, the frequency bands examined (theta and alpha) are least likely to be contaminated by EMG activity during challenging balance tasks, compared with beta and gamma bands.

Theta power

In contrast to previous work demonstrating an increase in theta power as a function of task difficulty in central and parietal regions (Hülsdünker et al., 2015; Hülsdünker et al., 2016), discussed further below, our data showed no association between task difficulty and theta power. However, Figs. 2 and 4 suggest a slight reduction in theta power during the postural tasks, with the exception of Cz. Given that theta oscillations are understood to be important during transient balance perturbations (Slobounov et al., 2009; Sipp et al., 2013; Slobounov et al., 2013; Varghese et al., 2014), a possible explanation for this discrepancy is that there are multiple, opposing event-sensitive changes in theta power that are not reflected in summary measurements of power in ‘‘steady-state”, continuous balance. Evidence exists to support this concept. Contrary changes in theta activity have been reported, depending upon both phase of balance and predictability of postural perturbation (Slobounov et al., 2009; Slobounov et al., 2013). Also, a locomotor study found that the theta increases in bilateral sensorimotor areas at the point of loss of balance are not seen during stable balance phases (Sipp et al., 2013).

However, as mentioned, our findings differ from those of Hülsdünker et al. (2015), who demonstrated an increase in theta power with increasing task difficulty in fronto-central and centro-parietal regions during continuous balance. In that study, as groups of at least 6 electrodes overlying midline, left and right cortical areas were analyzed together, it is possible that there are individual loci within this group at which there is no significant change in theta power, as we have found (C3, C4, P3, P4) [Figs. 2 and 4]. Despite no main effect of task difficulty on theta power and no significant correlations with rated difficulty, we observed that theta power at electrode Cz tended to increase with task difficulty until the most challenging task, at which there was a relative reduction (RFLOOR-RFOAM) [Figs. 2, 4 and 5]. The change at this electrode corresponds with the findings of Hülsdünker et al. (2015), who observed theta power increase across a widespread centro-parietal cortical area and described a similar ‘‘ceiling effect” of extreme balance difficulty. Disparity between these results and ours may be accounted for by the effect of grouping electrodes for analysis (Hülsdünker et al., 2015), rather than interrogation of activity at single electrode positions as we have done.

In any case, the pattern of theta activity in Cz differs from other surrounding electrodes, suggesting a distinct role for this cortical region, which corresponds to the

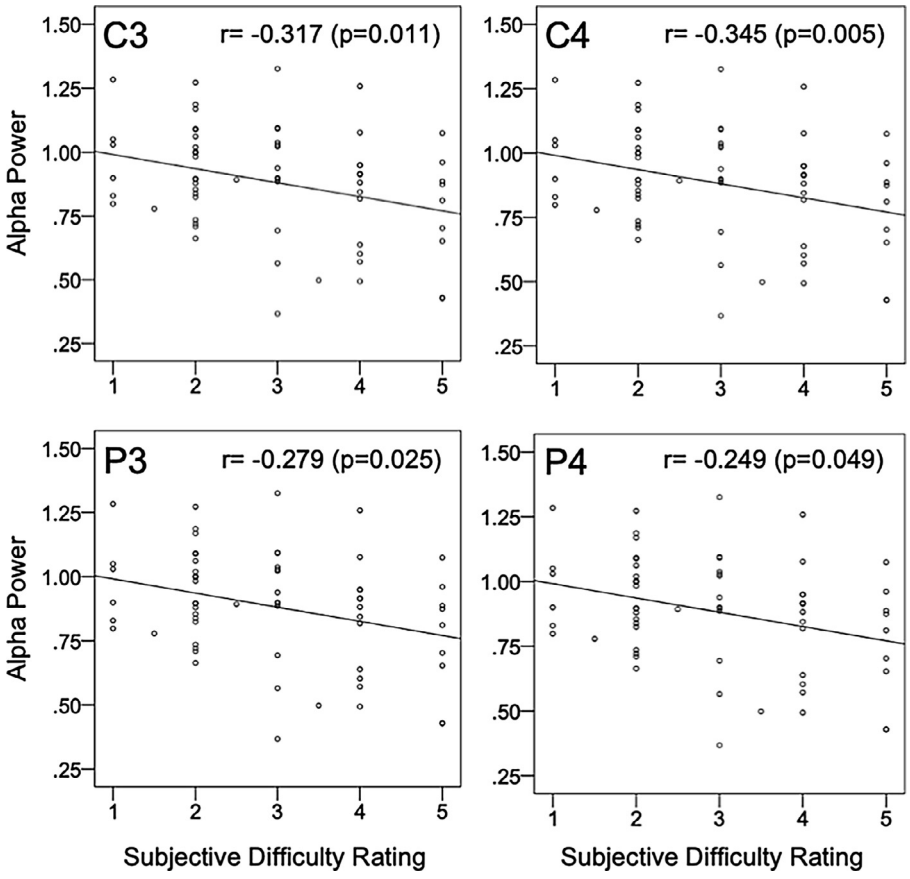

Fig. 6. Scatter plots demonstrating significant negative correlations between individual (n = 16) subjective task difficulty ratings (1–5) and relative power in the alpha frequency band: electrodes C3, C4, P3, P4 (top left to bottom right). Each plot displays individual values for 4 balance tasks with regression lines. Pearson correlation coefficients (r) and p-values are shown in the top right corner of each plot.

medial aspect of the primary motor cortex or "leg area" (Homan et al., 1987; Koessler et al., 2009). It is possible that the increased theta activity in this area represents a true surge in neural activity of the primary motor cortex, for example in adaptive postural activity while maintaining continuous balance. This interpretation agrees with views that theta oscillations could represent error detection and processing (Adkin et al., 2006; Slobounov et al., 2009; Varghese et al., 2015), as adaptive motor responses form the efferent component of these feedback loops. Alternatively, as there are strong functional connections between motor and parietal cortices (Koch et al., 2008; Feurra et al., 2011), the latter of which implicate vestibular functions (Dieterich et al., 2003b), it is also possible that the increase in theta power in Cz could reflect enhanced parieto-motor communication (Dieterich et al., 2003a). However, this latter hypothesis is not directly supported by our coherence data (showing coherence increase with task difficulty in central-central but not in central-parietal electrodes, albeit in the alpha band). Irrespective, separating afferent from efferent components during EEG experiments in freely moving subjects is notoriously difficult, and further studies in patients devoid of vestibular or proprioceptive function are underway to clarify this point. In addition, source localization with high-density EEG (Freeman et al., 2003; Song et al., 2015) and subject-specific MRI (Gohel et al., 2017), which we were not able to implement, should aid localizing accuracy.

The reduction in Cz theta power at the most extreme level of balance difficulty supports the suggestion of a "ceiling effect" for theta power in the leg motor area when postural instability becomes excessive (Hülsdünker et al., 2015). It is possible that beyond a certain level of unsteadiness, the balance function subserved by theta oscillations is taken over by other cortical or subcortical domains. Such a suggestion has previously been made only in relation to alpha and higher frequency bands (Tse et al., 2013). One could argue that such a shift could potentially explain postural instability in some elderly patients, as age-related deterioration of subcortical control loops and increasing reliance on cortical mechanisms has been postulated (Baudry, 2016; Ozdemir et al., 2018). However, a shift in power spectral distribution to higher frequencies when balance becomes extremely difficult is an alternative possibility. So far, there has been limited investigation of beta (12–30 Hz) and low gamma (30–40 Hz) power during continuous balance, and no investigation of frequencies above 50 Hz (Ozdemir et al., 2018). High-gamma (60–100 Hz) activity has been demonstrated in the primary motor cortex during voluntary movement and hypothesized to reflect cortico-subcortical feedback control (Cheyne et al., 2008). For this reason, frequencies above 60 Hz would be worth investigating in future EEG study of balance, although EMG contamination may be inevitable.

Theta power asymmetry

We also demonstrated significant hemispheric asymmetry in theta power, highlighted by significant differences between Cz and right-sided electrodes (C4, P4) and between left and right central electrodes (C3, C4) [Fig. 2]. Theta power was relatively lower in right-sided than left-sided central and parietal regions during all balance tasks [Fig. 4]. As this relative difference between the hemispheres is not limited to unipedal tasks, we can assume that it is not attributable to asymmetric leg activity. It is known that the vestibular cortex comprises several distinct regions including part of the posterior parietal cortex (Lopez and Blanke, 2011; Lopez et al., 2012), and that spatial functions are lateralized to the right hemisphere in right-handed people

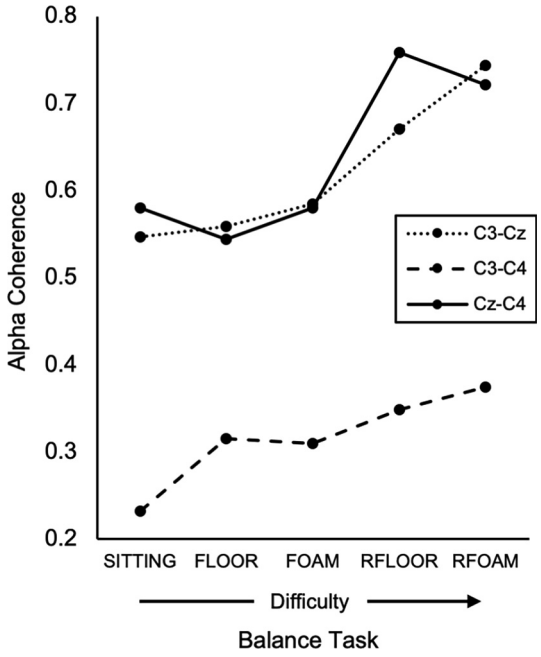

Fig. 7. Association between postural task (presented in order of increasing difficulty) and coherence in the alpha frequency band between central electrode pairs. For simplicity, median coherence values (n = 16) are shown for each task; in-text statistical correlations are between individual ratings of subjective task difficulty and individual inter-electrode coherence values normalized to SITTING (n = 16; all $p < 0.05$).

(Dieterich et al., 2003a; Janzen et al., 2008; Arshad et al., 2013; Nigmatullina et al., 2016). The relatively lower theta power at right parietal loci versus left could therefore represent greater feedback processing and spatial planning by spatial-dominant cortical areas, possibly by spectral shift to higher frequencies.

However, this interpretation may not necessarily account for asymmetry in central areas (C3–C4), which is more prominent. It is likely that electrodes C3 and C4 also overlie parts of the primary somatosensory cortex (Penfield and Rasmussen, 1957; de Klerk et al., 2015). Although this in itself does not provide a clear reason for hemispheric asymmetry, there is evidence that parts of the primary somatosensory cortex (Brodmann areas 3/1/2) close to these electrodes have properties linked to vestibular function (Urasaki and Yokota, 2003; Lopez and Blanke, 2011). Therefore, lower theta activity in C4 than C3 could represent greater multimodal sensory information processing by the spatial-dominant right hemisphere in central regions, in addition to parietal, as further supported by the notion of a distributed vestibular cortical network (Arshad, 2017).

Alpha power

Alpha power decreased significantly with increasing task difficulty in right and left-sided central and parietal areas. Alpha activity is understood to reflect inhibition of task-irrelevant brain regions, meaning alpha desynchronization (power reduction) represents increased information processing due to inhibition reduction by higher centres (Ray and Cole, 1985; Boiten et al., 1992; Del Percio et al., 2007; Slobounov et al., 2008; Klimesch, 2012; Babiloni et al., 2014). Our results therefore suggest that bilateral central and parietal cortical regions are functionally engaged in continuous balance control, and that information processing at these loci increases with balance challenge. Reductions in lower (8–10 Hz) and upper (10–12 Hz) alpha power with increasing postural sway during continuous balance have been previously reported across the centro-parietal region, suggesting involvement in balance control processes (Hülsdünker et al., 2016). However, this phenomenon had not been demonstrated consistently (Tse et al., 2013), possibly due to differences in balance task, spatial resolution, ROIs examined and a combination of external postural perturbation and sustained task investigations. Our findings support those of Hülsdünker et al. (2016), providing further indication that central and parietal alpha power reduction reflects increasing functional involvement of these areas with continuous balance challenge.

In parietal regions, observed alpha reductions may relate to increased external sensory attention and information processing, as previously postulated (Ray and Cole, 1985). That is, alpha power has been shown to be lower in tasks that involve sensory-intake than those that do not and is hypothesized to reflect greater external sensory attention (Ray and Cole, 1985). Notably, evidence for this external sensory attention concept of parietal alpha reduction has come from studies involving no motor response or somatosensory stimulation (Ray and Cole, 1985; Benedek et al., 2014). This would imply that the underlying changes in external sensory attention in parietal cortex only concern visuo-spatial, and not sensorimotor, attention. Thus, the reductions in parietal alpha power we found could reflect increases in vestibulo-spatial sensory attention with increasing balance demand, as visual input has been eliminated. Our novel finding that this active reduction in alpha activity is more prominent on the right in right-handed subjects fully supports this view, given that the spatial-attentional network is significantly lateralized to the non-dominant, right hemisphere (Karnath and Dieterich, 2006; Arshad et al., 2013; Arshad et al., 2015).

Bilateral parietal alpha suppression has also been demonstrated during rotational vestibular stimulation while sitting (Gale et al., 2016). Gale et al. (2016) made efforts to exclude somatosensory and proprioceptive involvement and comparisons were made between subjects with and without vestibular function, making the observed alpha suppression likely to reflect true vestibular cortical processing in parietal regions. This is also supportive of our observed parietal alpha power reduction indicating increasing activity of vestibulo-spatial parietal cortex as balance challenge increases.

We also demonstrate similar, more prominent, changes in central regions, not previously reported at this spatial resolution (Hülsdünker et al., 2016). This could imply that central changes also reflect increases in sensory rather than motor information processing, relating to areas of primary somatosensory cortex concerned with

vestibular function (Urasaki and Yokota, 2003; Lopez and Blanke, 2011). So, these changes, in parallel with parietal regions, may reflect increasing neural activity within multimodal sensory cortical networks with progressive balance task difficulty. However, the finding that alpha coherence between central-central but not central-parietal or parietal-parietal electrode pairs increases with task difficulty could represent the increased motor or sensorimotor co-processing required to deliver the motor component of the task. That said, differentiating sensory from motor processing is challenging, as already mentioned, and this topic will require further work in patients deprived of specific sensory inputs.

While reduction in alpha power with task difficulty was also seen in Cz [Fig. 3], the relationship here was not significant. As in the theta band, this difference suggests a distinct functional role for this cortical area in balance control, and perhaps further evidence that it is more reflective of leg motor activity than sensory processing. This interpretation is consistent with the concept that negative correlations between alpha power and task difficulty in bilateral central and parietal regions are indicative of increasing vestibular and multimodal sensory processing. Although a limitation of our study is not having yet studied patients with absent vestibular function, what we do know, on the basis of pilot studies, clinical experience and evidence in the literature (Honegger et al., 2013; Sprenger et al., 2017), is that the postural tasks explored here require intact vestibular function as they cannot be accomplished by avestibular patients.

Alpha power asymmetry

We also identified hemispheric asymmetry in the alpha band. As in the theta band, alpha power was relatively lower in right central and parietal regions than left during all balance tasks [Figs. 3 and 4]. This hemispheric asymmetry was most prominent between central electrodes [Fig. 4]. Asymmetry in alpha desynchronization has been widely reported during visual spatial attention (Sauseng, et al., 2005; Rihs et al., 2007; Feurra et al., 2011; Capotosto et al., 2012). As visual contribution to balance was excluded in our paradigm, the alpha hemispheric asymmetry may relate to sensorimotor and/or vestibular processing. Asymmetric alpha oscillations during walking have been reported to indicate fluctuating involvement of the sensorimotor cortex at different points during the gait cycle (Bradford et al., 2016). However, gait or stance-related sensorimotor involvement is unlikely to underlie alpha asymmetry in this study, as asymmetry persisted in bipedal as well as unipedal conditions. Previous work has also established that changes in alpha power do not take place during either passive or supported changes in body position (Chang et al., 2011; Thibault et al., 2014). This suggests that the asymmetry relates to more complex vestibulo-spatial functions, in keeping with our proposition that alpha reduction in parietal cortex corresponds to increasing vestibular cortical processing; we would expect that such activity, and alpha reduction, would be greater in the vestibular-dominant right hemisphere. Interestingly, passive vestibular stimulation induces no asymmetry in temporo-parietal alpha power (Gale et al., 2016), indicating that parietal vestibular hemispheric asymmetry must be specific to active balance control, and not simply sensory-intake and reflex circuit activation. This interpretation, when applied to more prominent central alpha asymmetry, would further support our suggestion that central areas overlie primary somatosensory cortex with vestibular functional connections.

To conclude, our findings illustrate the functional importance of bilateral central and parietal cortices in balance control, associated with increasing task difficulty. The hemispheric asymmetry observed supports the notion that the non-dominant hemisphere is involved with online monitoring of postural control. Although the posterior parietal asymmetry found may relate to vestibular, somatosensory or multisensory feedback processing, we argue that the finding relates to active balance control, rather than simple sensory-intake or reflex circuit activation. Theta increases in Cz and enhanced alpha coherence in central electrodes may relate more directly to motor processing in the cortical leg representation area. Although technical restrictions such as lack of EEG source localization and MRI data somewhat temper conclusions we can make regarding exact cortical localization, the fact that EEG correlates of balance can be made in real time opens a new door in the assessment of patients with dizziness and balance disorders. In turn, investigations into the effects of selective sensorimotor and/or vestibular deficits in patients will help to more fully understand the cortical correlates of balance control.

FUNDING

This study was supported by the UK Medical Research Council (MR/J004685/1), the Dunhill Medical Trust (R481/0516), the Dix Foundation and the National Institute for Health Research (NIHR) Imperial Biomedical Research Centre.

ACKNOWLEDGMENTS

We thank Mowleesan Amaralingam for his help in data collection, Dave Buckwell for technical support, and Tobias Reichenbach, Octave Etard, Dario Farina, Michael Gresty and Nicoletta Nicolau for helpful advice.

AUTHOR CONTRIBUTIONS

QA & AMB conceptualized & supervised the study; AEE acquired data; AEE, OG & MDF analysed data; AEE & OG prepared figures for the manuscript; AEE & AMB wrote the manuscript; OG wrote technical methodology for the manuscript; QA edited the manuscript.

REFERENCES

Adkin A, Quant S, Maki B, McIlroy W (2006) Cortical responses associated with predictable and unpredictable compensatory balance reactions. Exp Brain Res 172:85–93.

Ahmad H, Cerchiai N, Mancuso M, Casani AP, Bronstein AM (2015) Are white matter abnormalities associated with ‘‘unexplained dizziness”? J Neurol Sci 358:428.
Arshad Q, Siddiqui S, Ramachandran S, Goga U, Bonsu A, Patel M, Roberts RE, Nigmatullina Y, et al. (2015) Right hemisphere dominance directly predicts both baseline V1 cortical excitability and the degree of top-down modulation exerted over low-level brain structures. Neuroscience 311:484–489.
Arshad Q (2017) Dynamic interhemispheric competition and vestibulo-cortical control in humans; A theoretical proposition. Neuroscience 353:26–41.
Arshad Q, Nigmatullina Y, Bronstein AM (2013) Handedness-related cortical modulation of the vestibular-ocular reflex. J Neurosci 33:3221.
Arshad Q, Nigmatullina Y, Roberts RE, Bhrugubanda V, Asavarut P, Bronstein AM (2014) Left Cathodal Trans-Cranial Direct Current Stimulation of the Parietal Cortex Leads to an Asymmetrical Modulation of the Vestibular-Ocular Reflex. Brain Stimul 7:85–91.
Babiloni C, Infarinato F, Marzano N, Iacoboni M, Dassù F, Soricelli A, Rossini P, Limatola C, et al. (2011) Intra-hemispheric functional coupling of alpha rhythms is related to golfer’s performance: a coherence EEG study. Int J Psychophysiol 82:260–268.
Babiloni C, Del Percio C, Arendt-Nielsen L, Soricelli A, Romani GL, Rossini PM, Capotosto P (2014) Cortical EEG alpha rhythms reflect task-specific somatosensory and motor interactions in humans. Clin Neurophysiol 125:1936–1945.
Baudry S (2016) Aging changes the contribution of spinal and corticospinal pathways to control balance. Exerc Sport Sci Rev 44:104–109.
Benedek M, Schickel RJ, Jauk E, Fink A, Neubauer AC (2014) Alpha power increases in right parietal cortex reflects focused internal attention. Neuropsychologia 56:393–400.
Boiten F, Sergeant J, Geuze R (1992) Event-related desynchronization: the effects of energetic and computational demands. Electroencephalogr Clin Neurophysiol 82:302–309.
Bolton DAE (2015) The role of the cerebral cortex in postural responses to externally induced perturbations. Neurosci Biobehav Rev 57:142–155.
Bolton DAE, Williams L, Staines WR, McIlroy WE (2012) Contribution of primary motor cortex to compensatory balance reactions. BMC Neurosci 13:102.
Bradford JC, Lukos JR, Ferris DP (2016) Electrocortical activity distinguishes between uphill and level walking in humans. J Neurophysiol 115:958.
Brandt T (2003) Vestibular cortex: its locations, functions and disorders. In: Vertigo – its multisensory syndromes. New York: Springer-Verlag. p. 219–231.
Britton J, Frey L, Hopp J, Korb P, Koubeissi M, Lievens W, Pestana-Knight E, St. Louis E (2016) The abnormal EEG. In: St. Louis E, Frey L, editors. Electroencephalography (EEG): an introductory text and atlas of normal and abnormal findings in adults, children, and infants. Chicago: American Epilepsy Society.
Capotosto P, Babiloni C, Romani GL, Corbetta M (2012) Differential contribution of right and left parietal cortex to the control of spatial attention: a simultaneous EEG-rTMS study. Cereb Cortex 22:446–454.
Chang L, Lin J, Lin C, Wu K, Wang Y, Kuo C (2011) Effect of body position on bilateral EEG alterations and their relationship with autonomic nervous modulation in normal subjects. Neurosci Lett 490:96–100.
Cheyne D, Bells S, Ferrari P, Gaetz W, Bostan AC (2008) Self-paced movements induce high-frequency gamma oscillations in primary motor cortex. Neuroimage 42:332–342.
de Klerk Carina CJM, Johnson MH, Southgate V (2015) An EEG study on the somatotopic organisation of sensorimotor cortex activation during action execution and observation in infancy. Dev Cogn Neurosci 15:1–10.
Del Percio C, Babiloni C, Marzano N, Iacoboni M, Infarinato F, Vecchio F, Lizio R, Aschieri P, et al. (2009) ‘‘Neural efficiency” of athletes’ brain for upright standing: a high-resolution EEG study. Brain Res Bull 79:193–200.
Del Percio C, Brancucci A, Bergami F, Marzano N, Fiore A, Di Ciolo E, Aschieri P, Lino A, et al. (2007) Cortical alpha rhythms are correlated with body sway during quiet open-eyes standing in athletes: a high-resolution EEG study. Neuroimage 36:822–829.
Dieterich M, Bense S, Lutz S, Drzezga A, Stephan T, Bartenstein P, Brandt T (2003a) Dominance for vestibular cortical function in the non-dominant hemisphere. Cereb Cortex 13:994–1007.
Dieterich M, Bense S, Stephan T, Yousry TA, Brandt T (2003b) fMRI signal increases and decreases in cortical areas during small-field optokinetic stimulation and central fixation. Exp Brain Res 148:117–127.
Fasold O, von Brevern M, Kuhberg M, Ploner CJ, Villringer A, Lempert T, Wenzel R (2002) Human vestibular cortex as identified with caloric stimulation in functional magnetic resonance imaging. Neuroimage 17:1384–1393.
Federolf P, Roos L, Nigg B (2013) Analysis of the multi-segmental postural movement strategies utilized in bipedal, tandem and one-leg stance as quantified by a principal component decomposition of marker coordinates. J Biomech 46:2626–2633.
Feurra M, Bianco G, Polizzotto NR, Innocenti I, Rossi A, Rossi S (2011) Cortico-cortical connectivity between right parietal and bilateral primary motor cortices during imagined and observed actions: a combined TMS/tDCS study. Front Neural Circuits 5:10.
Freeman WJ, Holmes MD, Burke BC, Vanhatalo S (2003) Spatial spectra of scalp EEG and EMG from awake humans. Clin Neurophysiol 114:1053–1068.
Gale S, Prsa M, Schurger A, Gay A, Paillard A, Herbelin B, Guyot J, Lopez C, et al. (2016) Oscillatory neural responses evoked by natural vestibular stimuli in humans. J Neurophysiol 115:1228–1242.
Gevins A, Smith M (2000) Neurophysiological measures of working memory and individual differences in cognitive ability and cognitive style. Cereb Cortex 10:829–839.
Gohel B, Lim S, Kim MY, Kwon S, Kim K (2017) Approximate subject specific pseudo MRI from an available MRI dataset for MEG source imaging. Fronti Neuroinform 8:50.
Gomarus K, Althaus M, Wijers A, Minderaa R (2006) The effects of memory load and stimulus relevance on the EEG during a visual selective memory search task: an ERP and ERD/ERS study. Clin Neurophysiol 117:871–884.
Guerraz M, Yardley L, Bertholon P, Pollak L, Rudge P, Gresty MA, Bronstein AM (2001) Visual vertigo: symptom assessment, spatial orientation and postural control. Brain 124:1646–1656.
Harmony T, Fernández T, Silva J, Bernal J, Díaz-Comas L, Reyes A, Marosi E, Rodríguez M (1996) EEG delta activity: an indicator of attention to internal processing during performance of mental tasks. Int J Psychophysiol 24:161–171.
Homan RW, Herman J, Purdy P (1987) Cerebral location of international 10–20 system electrode placement. Electroencephalogr Clin Neurophysiol 66:376–382.
Honegger F, Hillebrandt IMA, van den Elzen Nadja GA, Tang K, Allum JHJ (2013) The effect of prosthetic feedback on the strategies and synergies used by vestibular loss subjects to control stance. J Neuroeng and Rehabil 10:115.
Hülsdünker T, Mierau A, Neeb C, Kleinöder H, Strüder HK (2015) Cortical processes associated with continuous balance control as revealed by EEG spectral power. Neurosci Lett 59:1–5.
Hülsdünker T, Mierau A, Strüder HK (2016) Higher balance task demands are associated with an increase in individual alpha peak frequency. Front Hum Neurosci 9:695.
Jacobs JV, Horak FB (2007) Cortical control of postural responses. J Neural Transm 114:1339–1348.
Janzen J, Schlindwein P, Bense S, Bauermann T, Vucurevic G, Stoeter P, Dieterich M (2008) Neural correlates of hemispheric dominance and ipsilaterality within the vestibular system. Neuroimage 42:1508.
Kahane P, Hoffmann D, Minotti L, Berthoz A (2003) Reappraisal of the human vestibular cortex by cortical electrical stimulation study. Ann Neurol 54:615–624.
Kalaska JF, Cohen DA, Prud’homme M, Hyde ML (1990) Parietal area 5 neuronal activity encodes movement kinematics, not movement dynamics. Exp Brain Res 80:351.

Karnath HO, Dieterich M (2006) Spatial neglect–a vestibular disorder? Brain 19:293–305.
Kaski D, Quadir S, Nigmatullina Y, Malhotra PA, Bronstein AM, Seemungal BM (2016) Temporoparietal encoding of space and time during vestibular-guided orientation. Brain 139:392–403.
Keck ME, Pijnappels M, Schubert M, Colombo G, Curt A, Dietz V (1998) Stumbling reactions in man: influence of corticospinal input. Electroencephalogr Clin Neurophysiol 109:215–223.
Kim H, Yi H, Lee H (2015) Recent advances in orthostatic hypotension presenting orthostatic dizziness or vertigo. Neurol Sci 36:1995–2002.
Klimesch W (2012) Alpha-band oscillations, attention, and controlled access to stored information. Trends Cogn Sci 16:606–617.
Koch G, Del Olmo MF, Cheeran B, Schippling S, Caltagirone C, Driver J, Rothwell JC (2008) Functional interplay between posterior parietal and ipsilateral motor cortex revealed by twin-coil transcranial magnetic stimulation during reach planning toward contralateral space. J Neurosci 28:5944–5953.
Koessler L, Maillard L, Benhadid A, Vignal JP, Felblinger J, Vespignani H, Braun M (2009) Automated cortical projection of EEG sensors: anatomical correlation via the international 10–10 system. Neuroimage 46:64–72.
Lekhel H, Popov K, Anastasopoulos D, Bronstein AM, Bhatia K, Marsden CD, Gresty MA (1997) Postural responses to vibration of neck muscles in patients with idiopathic torticollis. Brain 120(Pt 4):583–591.
Limanowski J, Blankenburg F (2016) Integration of visual and proprioceptive limb position information in human posterior parietal, premotor, and extrastriate cortex. J Neurosci 36:2582–2589.
Lopez C, Blanke O, Mast FW (2012) The human vestibular cortex revealed by coordinate-based activation likelihood estimation meta-analysis. Neuroscience 212:159–179.
Lopez C, Blanke O (2011) The thalamocortical vestibular system in animals and humans. Brain Res Rev 67:119–146.
Magnus R (1926) Physiology of posture. Lancet 11:531–585.
Maurer C, Mergner T, Bolha B, Hlavacka F (2000) Vestibular, visual, and somatosensory contributions to human control of upright stance. Neurosci Lett 281:99–102.
Mihara M, Miyai I, Hatakenaka M, Kubota K, Sakoda S (2008) Role of the prefrontal cortex in human balance control. Neuroimage 43:329–336.
Nigmatullina Y, Siddiqui S, Khan S, Sander K, Lobo R, Bronstein AM, Arshad Q (2016) Lateralisation of the vestibular cortex is more pronounced in left-handers. Brain Stimul 9:942–944.
Nigro S, Indovina I, Riccelli R, Chiarella G, Petrolo C, Lacquaniti F, Staab JP, Passamonti L (2018) Reduced cortical folding in multimodal vestibular regions in persistent postural perceptual dizziness. Brain Imaging Behav:1–12.
Okamoto M, Dan H, Sakamoto K, Takeo K, Shimizu K, Kohno S, Oda I, Isobe S, et al. (2004) Three-dimensional probabilistic anatomical cranio-cerebral correlation via the international 10–20 system oriented for transcranial functional brain mapping. Neuroimage 21:99–111.
Ouchi Y, Okada H, Yoshikawa E, Nobezawa S, Futatsubashi M (1999) Brain activation during maintenance of standing postures in humans. Brain 122:329–338.
Ozdemir RA, Contreras-Vidal JL, Paloski WH (2018) Cortical control of human upright stance in elderly. Mech Ageing Dev 169:19–31.
Pellijeff A, Bonilha L, Morgan PS, McKenzie K, Jackson SR (2006) Parietal updating of limb posture: an event-related fMRI study. Neuropsychologia 44:2685–2690.
Penfield W, Rasmussen T (1957) The cerebral cortex of man. New York U.A.: Macmillan.
Pfurtscheller G, Neuper C, Krausz G (2000) Functional dissociation of lower and upper frequency mu rhythms in relation to voluntary limb movement. Clin Neurophysiol 111:1873–1879.
Pérrenou DA, Mazibrada G, Chauvineau V, Greenwood R, Rothwell J, Gresty MA, et al. (2008) Lateropulsion, pushing and verticality perception in hemisphere stroke: a causal relationship? Brain 131:2401–2413.
Ray WJ, Cole HW (1985) EEG alpha activity reflects attentional demands, and beta activity reflects emotional and cognitive processes. Science 228(4700):750–752.
Rihs TA, Michel CM, Thut G (2007) Mechanisms of selective inhibition in visual spatial attention are indexed by alpha-band EEG synchronization. Eur J Neurosci 25:603–610.
Sauseng P, Klimesch W, Stadler W, Schabus M, Doppelmayr M, Hanslmayr S, Gruber WR, Birbaumer N (2005) A shift of visual spatial attention is selectively associated with human EEG alpha activity. Eur J Neurosci 22:2917–2926.
Sauseng P, Gerloff C, Hummel FC (2013) Two brakes are better than one: the neural bases of inhibitory control of motor memory traces. Neuroimage 65:52–58.
Schöberl F, Feil K, Xiong G, Bartenstein P, la Fougére C, Jahn K, Brandt T, Strupp M, et al. (2017) Pathological ponto-cerebello-thalamo-cortical activations in primary orthostatic tremor during lying and stance. Brain 140:83–97.
Scott D (1976) Chapter 2: the normal and abnormal EEG. In: Understanding EEG. London: Gerald Duckworth & Co., Ltd.. p. 18–32.
Sipp AR, Gwin JT, Makeig S, Ferris DP (2013) Loss of balance during balance beam walking elicits a multifocal theta band electrocortical response. J Neurophysiol 110:2050–2060.
Slobounov S, Hallett M, Stanhope S, Shibasaki H (2005) Role of cerebral cortex in human postural control: an EEG study. Clin Neurophysiol 116:315–323.
Slobounov S, Tutwiler R, Slobounova E, Rearick M, Ray W (2000) Human oscillatory brain activity within gamma band (30–50 Hz) induced by visual recognition of non-stable postures. Cogn Brain Res 9:177–192.
Slobounov SM, Teel E, Newell KM (2013) Modulation of cortical activity in response to visually induced postural perturbation: combined VR and EEG study. Neurosci Lett 547:6.
Slobounov S, Cao C, Jaiswal N, Newell KM (2009) Neural basis of postural instability identified by VTC and EEG. Exp Brain Res 199:1–16.
Slobounov S, Hallett M, Cao C, Newell K (2008) Modulation of cortical activity as a result of voluntary postural sway direction: an EEG study. Neurosci Lett 442(3):309–313.
Song J, Davey C, Poulson C, Luu P, Turovets S, Anderson E, Li K, Tucker D (2015) EEG source localization: sensor density and head surface coverage. J Neurosci Methods 30:9–21.
Sprenger A, Wojak JF, Jandl NM, Helmchen C (2017) Postural control in bilateral vestibular failure: its relation to visual, proprioceptive, vestibular, and cognitive input. Front Neurol 1(8):444.
Thibault RT, Lifshitz M, Jones JM, Raz A (2014) Posture alters human resting-state. Cortex 58:199–205.
Trans Cranial Technologies (2012) Cortical Functions. Hong Kong: Trans Cranial Technologies ltd.
Tse YYF, Petrofsky JS, Berk L, Daher N, Lohman E, Laymon MS, Cavalcanti P (2013) Postural sway and Rhythmic Electroencephalography analysis of cortical activation during eight balance training tasks. Med Sci Monit 19:175.
Urasaki E, Yokota A (2003) Vertigo and dizziness associated with cerebral hemispheric lesions. J UOEH 25:207.
Varghese JP, Beyer KB, Williams L, Miyasike-daSilva V, McIlroy WE (2015) Standing still: is there a role for the cortex? Neurosci Lett 590:18–23.
Varghese JP, Marlin A, Beyer KB, Staines WR, Mochizuki G, McIlroy WE (2014) Frequency characteristics of cortical activity associated with perturbations to upright stability. Neurosci Lett 578:33–38.
Wang Y, Hong B, Gao X, Gao S (2006) Phase Synchrony Measurement in Motor Cortex for Classifying Single-trial EEG during motor Imagery. Ann Int Conf IEEE Eng Med Biol Soc:75–78.
Widmann A, Schröger E (2012) Filter effects and filter artifacts in the analysis of electrophysiological data. Front Psychol 3:233.
Widmann A, Schröger E, Maess B (2015) Digital filter design for electrophysiological data – a practical approach. J Neurosci Methods 250:34–46.

Yarrow K, Brown P, Gresty MA, Bronstein AM (2001) Force platform recordings in the diagnosis of primary orthostatic tremor. Gait Posture 13:27–34.
zu Eulenburg P, Caspers S, Roski C, Eickhoff SB (2012) Meta-analytical definition and functional connectivity of the human vestibular cortex. Neuroimage 60:162–169.

APPENDIX

Appendix 1. Coherence data: mean and median values for alpha (n = 16) and theta (n = 20) coherence.

Table A.1. Mean alpha coherence values between electrode pairs

SITTING	C3	C4	Cz	P3	P4
C3	1	0.3292	0.5977	0.4962	0.4548
C4	0.3292	1	0.6212	0.3915	0.4093
Cz	0.5977	0.6212	1	0.399	0.4011
P3	0.4962	0.3915	0.399	1	0.3206
P4	0.4548	0.4093	0.4011	0.3206	1
FLOOR	C3	C4	Cz	P3	P4
C3	1	0.3728	0.6097	0.5301	0.4423
C4	0.3728	1	0.5992	0.3848	0.4428
Cz	0.6097	0.5992	1	0.3995	0.3752
P3	0.5301	0.3848	0.3995	1	0.3224
P4	0.4423	0.4428	0.3752	0.3224	1
FOAM	C3	C4	Cz	P3	P4
C3	1	0.3746	0.6641	0.5166	0.4708
C4	0.3746	1	0.634	0.4078	0.4641
Cz	0.6641	0.634	1	0.3945	0.3846
P3	0.5166	0.4078	0.3945	1	0.3122
P4	0.4708	0.4641	0.3846	0.3122	1
RFLOOR	C3	C4	Cz	P3	P4
C3	1	0.4322	0.679	0.4925	0.4793
C4	0.4322	1	0.6893	0.4182	0.4393
Cz	0.679	0.6893	1	0.4031	0.4218
P3	0.4925	0.4182	0.4031	1	0.3533
P4	0.4793	0.4393	0.4218	0.3533	1
RFOAM	C3	C4	Cz	P3	P4
C3	1	0.4193	0.7216	0.4298	0.5131
C4	0.4193	1	0.6846	0.4254	0.4089
Cz	0.7216	0.6846	1	0.3781	0.4309
P3	0.4298	0.4254	0.3781	1	0.2895
P4	0.5131	0.4089	0.4309	0.2895	1

Table A.2. Median alpha coherence values between electrode pairs

SITTING	C3	C4	Cz	P3	P4
C3	1	0.2325	0.5466	0.4739	0.429
C4	0.2325	1	0.5799	0.3804	0.3789
Cz	0.5466	0.5799	1	0.3136	0.3792
P3	0.4739	0.3804	0.3136	1	0.2742
P4	0.429	0.3789	0.3792	0.2742	1
FLOOR	C3	C4	Cz	P3	P4
C3	1	0.3154	0.5591	0.5314	0.4452
C4	0.3154	1	0.544	0.3593	0.3756
Cz	0.5591	0.544	1	0.377	0.3118
P3	0.5314	0.3593	0.377	1	0.2244
P4	0.4452	0.3756	0.3118	0.2244	1
FOAM	C3	C4	Cz	P3	P4
C3	1	0.3099	0.5849	0.4913	0.4581
C4	0.3099	1	0.6376	0.3868	0.4483
Cz	0.5849	0.6376	1	0.349	0.4041
P3	0.4913	0.3868	0.349	1	0.2068
P4	0.4581	0.4483	0.4041	0.2068	1
RFLOOR	C3	C4	Cz	P3	P4
C3	1	0.3484	0.6704	0.5326	0.4458
C4	0.3484	1	0.7588	0.353	0.3962
Cz	0.6704	0.7588	1	0.3391	0.3972
P3	0.5326	0.353	0.3391	1	0.2877
P4	0.4458	0.3962	0.3972	0.2877	1
RFOAM	C3	C4	Cz	P3	P4
C3	1	0.3742	0.7441	0.3969	0.4918
C4	0.3742	1	0.7214	0.3975	0.3644
Cz	0.7441	0.7214	1	0.3217	0.4005
P3	0.3969	0.3975	0.3217	1	0.1843
P4	0.4918	0.3644	0.4005	0.1843	1

Table A.3. Mean theta coherence values between electrode pairs

SITTING	C3	C4	Cz	P3	P4
C3	1	0.2785	0.5353	0.4306	0.2675
C4	0.2785	1	0.6065	0.2433	0.3426
Cz	0.5353	0.6065	1	0.2801	0.2722
P3	0.4306	0.2433	0.2801	1	0.2308
P4	0.2675	0.3426	0.2722	0.2308	1
FLOOR	C3	C4	Cz	P3	P4
C3	1	0.2524	0.5502	0.4306	0.2388
C4	0.2524	1	0.576	0.216	0.3408
Cz	0.5502	0.576	1	0.2155	0.2047
P3	0.4306	0.216	0.2155	1	0.2116
P4	0.2388	0.3408	0.2047	0.2116	1
FOAM	C3	C4	Cz	P3	P4
C3	1	0.2597	0.5601	0.395	0.2446
C4	0.2597	1	0.5793	0.2123	0.3313
Cz	0.5601	0.5793	1	0.2178	0.228
P3	0.395	0.2123	0.2178	1	0.224
P4	0.2446	0.3313	0.228	0.224	1

(*continued on next page*)

Table A.3 (*continued*)

RFLOOR	C3	C4	Cz	P3	P4
C3	1	0.3348	0.6083	0.4224	0.2548
C4	0.3348	1	0.6313	0.2269	0.3718
Cz	0.6083	0.6313	1	0.2712	0.2557
P3	0.4224	0.2269	0.2712	1	0.2768
P4	0.2548	0.3718	0.2557	0.2768	1
RFOAM	C3	C4	Cz	P3	P4
C3	1	0.2768	0.5709	0.4495	0.2875
C4	0.2768	1	0.6058	0.2419	0.3721
Cz	0.5709	0.6058	1	0.2985	0.2859
P3	0.4495	0.2419	0.2985	1	0.2889
P4	0.2875	0.3721	0.2859	0.2889	1

Table A.4. Median theta coherence values between electrode pairs

SITTING	C3	C4	Cz	P3	P4
C3	1	0.1976	0.4751	0.4108	0.2147
C4	0.1976	1	0.5712	0.2376	0.2814
Cz	0.4751	0.5712	1	0.197	0.1633
P3	0.4108	0.2376	0.197	1	0.1904
P4	0.2147	0.2814	0.1633	0.1904	1
FLOOR	C3	C4	Cz	P3	P4
C3	1	0.1478	0.4883	0.4203	0.1819
C4	0.1478	1	0.5406	0.1911	0.2881
Cz	0.4883	0.5406	1	0.1533	0.1232
P3	0.4203	0.1911	0.1533	1	0.2129
P4	0.1819	0.2881	0.1232	0.2129	1
FOAM	C3	C4	Cz	P3	P4
C3	1	0.1749	0.5416	0.3638	0.1699
C4	0.1749	1	0.5083	0.1813	0.3038
Cz	0.5416	0.5083	1	0.1388	0.1638
P3	0.3638	0.1813	0.1388	1	0.2109
P4	0.1699	0.3038	0.1638	0.2109	1
RFLOOR	C3	C4	Cz	P3	P4
C3	1	0.2305	0.6188	0.3598	0.1719
C4	0.2305	1	0.6415	0.1699	0.3447
Cz	0.6188	0.6415	1	0.1879	0.1787
P3	0.3598	0.1699	0.1879	1	0.2554
P4	0.1719	0.3447	0.1787	0.2554	1
RFOAM	C3	C4	Cz	P3	P4
C3	1	0.1212	0.4885	0.396	0.2146
C4	0.1212	1	0.5596	0.1404	0.2981
Cz	0.4885	0.5596	1	0.2011	0.1733
P3	0.396	0.1404	0.2011	1	0.221
P4	0.2146	0.2981	0.1733	0.221	1

(Received 10 August 2018, Accepted 23 October 2018)
(Available online 01 November 2018)